

# Chemistry of $[\text{RuL}_2(\text{PPh}_3)_2]^{0,+}$ (HL = 8-hydroxyquinoline): Synthesis, Structure, Metal Redox Behaviour and Isomer Selectivity†

Mahua Menon, Amitava Pramanik, Nilkamal Bag and Animesh Chakravorty\*

Department of Inorganic Chemistry, Indian Association for the Cultivation of Science, Calcutta 700032, India

The reaction of  $[\text{Ru}(\text{PPh}_3)_3\text{Cl}_2]$  with 8-hydroxyquinoline (HL) has afforded  $[\text{RuL}_2(\text{PPh}_3)_2]$  in two isomeric forms, one red and one yellow-green, the  $\text{RuN}_2\text{O}_2\text{P}_2$  co-ordination sphere being *cis,trans,cis* and *trans,trans,trans* respectively. Chemical or electrochemical oxidation of either isomer affords exclusively red-brown *trans,trans,trans*- $[\text{RuL}_2(\text{PPh}_3)_2]^+$  isolated as the  $\text{PF}_6^-$  salt. The latter complex is one-electron paramagnetic (low-spin  $t_2^5$ ) and in frozen glass (77 K) displays a rhombic EPR spectrum. Reduction of *trans,trans,trans*- $[\text{RuL}_2(\text{PPh}_3)_2]\text{PF}_6$  by chemical or electrochemical means yields only *trans,trans,trans*- $[\text{RuL}_2(\text{PPh}_3)_2]$ . X-Ray crystallography has been performed on *cis,trans,cis*- $[\text{RuL}_2(\text{PPh}_3)_2]$  and *trans,trans,trans*- $[\text{RuL}_2(\text{PPh}_3)_2]\text{PF}_6\cdot\text{CH}_2\text{Cl}_2$ . The Ru–O and Ru–N bond lengths decrease upon metal oxidation but the Ru–P bond length increases by ca. 0.15 Å (strong  $4d\pi\text{--}3d\pi$  Ru<sup>III</sup>–P back-bonding). The reduction potential (Ru<sup>III</sup>–Ru<sup>II</sup>) order  $E_3(\text{cis,trans,cis}) > E_3(\text{trans,trans,trans})$  corresponds to superior back-bonding in the *cis*- as compared to the *trans*-Ru( $\text{PPh}_3$ )<sub>2</sub> motif. The stability of the observed geometry–valence combinations has been rationalised in terms of back-bonding, phosphine crowding and phenolato oxygen repulsion.

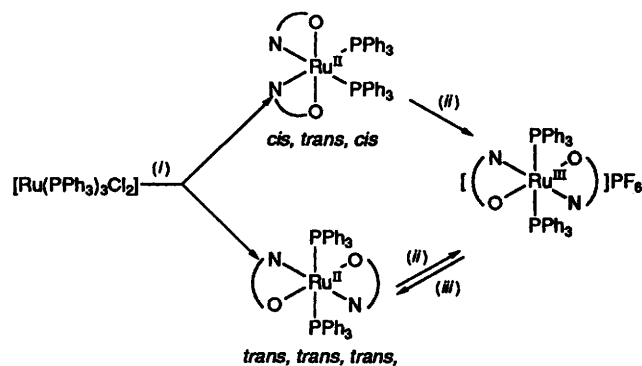
The selective stabilisation of geometrically isomeric co-ordination spheres by different oxidation states of the same metal ion is an important facet of variable-valence transition-metal chemistry.<sup>1–3</sup> In the particular case of ruthenium our studies have concerned the two possible isomeric forms *cis* and *trans*, in systems of the type  $[\text{RuL}'_2(\text{PPh}_3)_2]^z$  where L' is a monoanionic, symmetrical bidentate ligand being either an SS or an NN donor ( $z = 0$ , Ru<sup>II</sup>;  $z = +1$ , Ru<sup>III</sup>).<sup>4,5</sup> Upon replacing L' by an unsymmetrical, monoanionic bidentate ligand more isomeric forms become available for the oxidation states to choose from. This situation is explored in the present work using 8-hydroxyquinoline (HL) as the unsymmetrical ligand. The ON-chelating L<sup>–</sup> anion is known to have good affinity towards ruthenium.<sup>6–11</sup> Herein we report the isolation and characterisation of two isomeric forms of  $[\text{RuL}_2(\text{PPh}_3)_2]$  and of one form of  $[\text{RuL}_2(\text{PPh}_3)_2]\text{PF}_6$ . Structure determination of two of the species has clarified valence–geometry inter-relationships.

## Results and Discussion

**Synthesis and Characterisation.**—The synthesis of the species isolated in the present work are outlined in Scheme 1. The geometrical forms are defined by the relative positions (*cis* or *trans*) of the atoms within the co-ordination pairs NN, OO and PP taken in that order. The geometries in Scheme 1 have been revealed by X-ray and/or other studies (see below).

The two bivalent isomers of  $[\text{RuL}_2(\text{PPh}_3)_2]$ , red *cis,trans,cis* and yellow-green *trans,trans,trans* are formed in nearly equal proportions from the reaction of  $[\text{Ru}(\text{PPh}_3)_3\text{Cl}_2]$  and HL (no other isomers were formed even as minor constituents). The two isomers display remarkable thermal stability in solution and do not undergo any interconversion (as judged by spectral and electrochemical monitoring) even upon prolonged (several hours) boiling of solutions in dichloromethane, ethanol or acetonitrile.

Upon treatment with cerium(IV) the metal centre is oxidised.



**Scheme 1** (i) 8-Hydroxyquinoline, EtOH, reflux; (ii)  $\text{CH}_2\text{Cl}_2\text{--MeCN}$  (1:1),  $[\text{NH}_4]_4[\text{Ce}(\text{SO}_4)_4]\cdot 2\text{H}_2\text{O--H}_2\text{O}$ , stir,  $\text{NH}_4\text{PF}_6\text{--H}_2\text{O}$ ; (iii) MeCN,  $\text{H}_2\text{NNH}_2\cdot\text{H}_2\text{O}$ , stir

Both the *cis,trans,cis* and the *trans,trans,trans* isomers afford the same red-brown trivalent complex having exclusive *trans,trans,trans* geometry. It is isolated as the hexafluorophosphate (single crystals grown from dichloromethane–hexane contain a  $\text{CH}_2\text{Cl}_2$  molecule of crystallisation, see below). Evidently the bivalent *cis,trans,cis* complex is subject to oxidative isomerisation. Reduction of the trivalent *trans,trans,trans* complex by hydrazine hydrate proceeds quantitatively affording the bivalent *trans,trans,trans* isomer only; no *cis,trans,cis* isomer is formed in this process.

Selected characterisation data are given in Table 1. The diamagnetic bivalent isomers are non-electrolytic in nature whereas *trans,trans,trans*- $[\text{RuL}_2(\text{PPh}_3)_2]\text{PF}_6$  acts as a 1:1 electrolyte ( $\Lambda = 137 \Omega^{-1} \text{cm}^2 \text{mol}^{-1}$ ) in solution. Characteristic electronic spectral features are displayed in Fig. 1. The trivalent complex has an intense transition near 1000 nm presumably due to phenolato  $\rightarrow$  ruthenium(III) ligand-to-metal charge-transfer excitation. The complex has the expected  $S = \frac{1}{2}$  spin configuration (low-spin  $t_2^5$ ). Its X-band EPR spectrum in frozen (77 K) 1:1 dichloromethane–toluene glass is rhombic ( $g = 2.434, 2.054$  and  $1.878$ ) as expected ( $C_1$  symmetry of the co-ordination sphere, see below).

† Supplementary data available: see Instructions for Authors, *J. Chem. Soc., Dalton Trans.*, 1995, Issue 1, pp. xxv–xxx.

**Table 1** Analytical, electronic spectral and magnetic-moment data

Compound	Analysis <sup>a</sup> (%)			UV/VIS and NIR spectral data, $\lambda_{\text{max}}/\text{nm}$ ( $\epsilon/\text{dm}^3 \text{ mol}^{-1} \text{ cm}^{-1}$ ) <sup>b</sup>	$\mu_{\text{eff}}/\mu_{\text{B}}$
	C	H	N		
<i>cis,trans,cis</i> -[RuL <sub>2</sub> (PPh <sub>3</sub> ) <sub>2</sub> ]	70.8 (70.9)	4.5 (4.6)	3.0 (3.1)	480 (3075), 360 (6890)	Diamagnetic
<i>trans,trans,trans</i> -[RuL <sub>2</sub> (PPh <sub>3</sub> ) <sub>2</sub> ]	70.9 (70.9)	4.5 (4.6)	3.0 (3.1)	720 (sh) (2460), 550 (sh) (3460), 470 (7950), 330 (6800)	Diamagnetic
<i>trans,trans,trans</i> -[RuL <sub>2</sub> (PPh <sub>3</sub> ) <sub>2</sub> ]PF <sub>6</sub>	61.3 (61.2)	3.9 (4.0)	2.6 (2.6)	960 (4060), 550 (sh) (2050), 500 (sh) (2390), 390 (sh) (7820), 355 (8460)	1.87

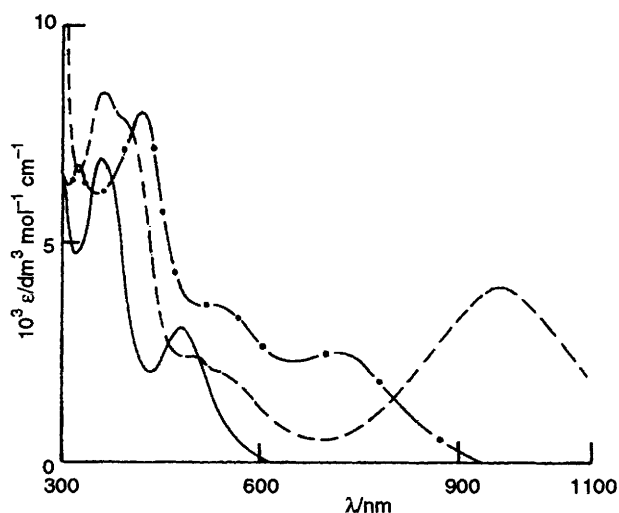
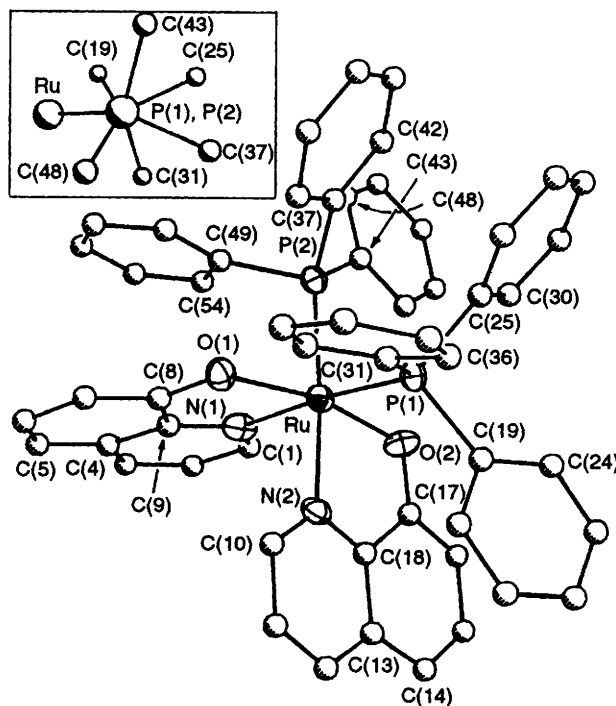
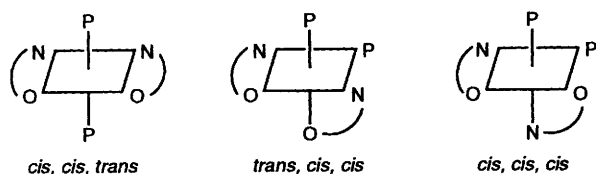
<sup>a</sup> Calculated values are in parentheses. <sup>b</sup> In dichloromethane at 298 K. <sup>c</sup> In the solid state at 298 K;  $\mu_{\text{B}} \approx 9.274 02 \times 10^{-24} \text{ J T}^{-1}$ .

**Table 2** Selected bond distances (Å) and angles (°) for *cis-trans-cis*-[RuL<sub>2</sub>(PPh<sub>3</sub>)<sub>2</sub>]

Ru–P(1)	2.322(3)	Ru–P(2)	2.327(3)
Ru–O(1)	2.090(6)	Ru–O(2)	2.099(6)
Ru–N(1)	2.096(8)	Ru–N(2)	2.089(9)
P(1)–Ru–P(2)	97.9(1)	P(1)–Ru–O(1)	98.8(2)
P(1)–Ru–O(2)	89.2(2)	P(1)–Ru–N(1)	174.0(2)
P(1)–Ru–N(2)	88.3(2)	P(2)–Ru–O(1)	88.6(2)
P(2)–Ru–O(2)	100.7(2)	P(2)–Ru–N(1)	87.9(2)
P(2)–Ru–N(2)	173.8(2)	O(1)–Ru–O(2)	166.9(3)
O(1)–Ru–N(1)	79.7(3)	O(1)–Ru–N(2)	89.9(3)
O(2)–Ru–N(1)	91.3(3)	O(2)–Ru–N(2)	79.8(3)
N(1)–Ru–N(2)	85.9(3)		

**Table 3** Selected bond distances (Å) and angles (°) for *trans,trans,trans*-[RuL<sub>2</sub>(PPh<sub>3</sub>)<sub>2</sub>]PF<sub>6</sub>·CH<sub>2</sub>Cl<sub>2</sub>

Ru(1)–P(1)	2.453(3)	Ru(2)–P(2)	2.522(3)
Ru(1)–O(1)	2.001(5)	Ru(2)–O(2)	1.996(6)
Ru(1)–N(1)	2.074(9)	Ru(2)–N(2)	2.063(9)
P(1)–Ru(1)–O(1)	86.3(2)	P(2)–Ru(2)–O(2)	96.3(2)
P(1)–Ru(1)–N(1)	88.7(2)	P(2)–Ru(2)–N(2)	87.9(2)
O(1)–Ru(1)–N(1)	81.1(3)	O(2)–Ru(2)–N(2)	80.4(3)

**Fig. 1** Electronic spectra of *cis,trans,cis*-[RuL<sub>2</sub>(PPh<sub>3</sub>)<sub>2</sub>] (—), *trans,trans,trans*-[RuL<sub>2</sub>(PPh<sub>3</sub>)<sub>2</sub>] (---) and *trans,trans,trans*-[RuL<sub>2</sub>(PPh<sub>3</sub>)<sub>2</sub>]PF<sub>6</sub> (— · —) in dichloromethane**Fig. 2** Perspective view and atom labelling scheme for *cis,trans,cis*-[RuL<sub>2</sub>(PPh<sub>3</sub>)<sub>2</sub>]. Inset: the two PC<sub>3</sub> fragments viewed down the PP axis

A red [Ru<sup>II</sup>L<sub>2</sub>(PPh<sub>3</sub>)<sub>2</sub>] complex prepared from [RuH<sub>2</sub>(PPh<sub>3</sub>)<sub>4</sub>] and HL was assigned (<sup>31</sup>P NMR) *cis,cis,trans* or *trans,trans,trans* geometry.<sup>6</sup> A repeat synthesis yielded the red complex as the major product and a yellow-green complex was also isolated in minor amounts. The red and yellow-green complexes are found to be identical in all respects with the *cis,trans,cis* (not *cis,cis,trans*) and *trans,trans,trans* forms, respectively, in Scheme 1.

**Crystal Structure.**—The geometry assignment of *cis,trans,cis*-[RuL<sub>2</sub>(PPh<sub>3</sub>)<sub>2</sub>] and *trans,trans,trans*-[RuL<sub>2</sub>(PPh<sub>3</sub>)<sub>2</sub>]PF<sub>6</sub>·CH<sub>2</sub>Cl<sub>2</sub> is based on X-ray structure determinations. Perspective views are shown in Figs. 2 and 3, and selected bond distances and angles are listed in Tables 2 and 3. There is no crystallographically imposed symmetry in *cis,trans,cis*-[RuL<sub>2</sub>(PPh<sub>3</sub>)<sub>2</sub>] but in *trans,trans,trans*-[RuL<sub>2</sub>(PPh<sub>3</sub>)<sub>2</sub>]<sup>+</sup> the metal atoms lie at crystallographic centres of inversion. The two crystallographically distinct but geometrically similar molecules constitute the unit cell. The PF<sub>6</sub><sup>−</sup> anion and the CH<sub>2</sub>Cl<sub>2</sub> molecule of crystallisation occupy general positions.

In both complexes the RuL fragments constitute good planes (mean deviation in the range 0.01–0.05 Å). The dihedral angle between the two RuL planes in *cis,trans,cis*-[RuL<sub>2</sub>(PPh<sub>3</sub>)<sub>2</sub>] is 83.2°. As is generally true for the *cis*-M(PPh<sub>3</sub>)<sub>2</sub> fragment in

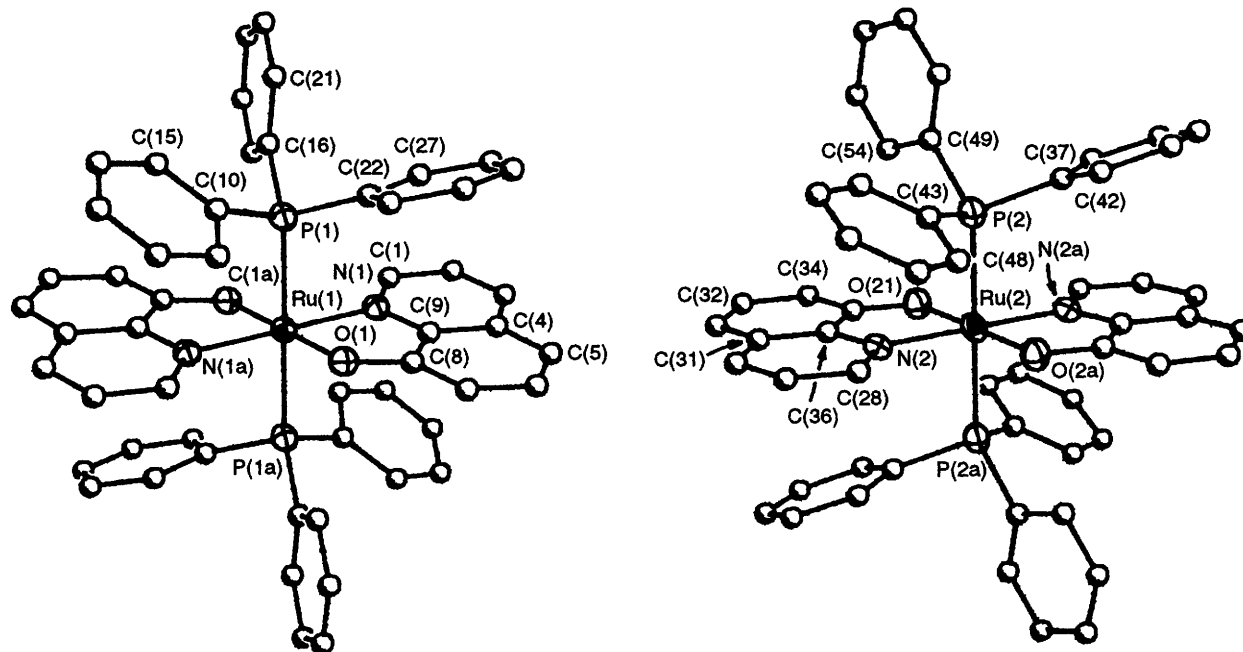


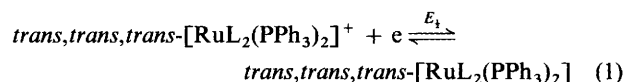
Fig. 3 Perspective view and atom labelling scheme for the two independent cations of *trans,trans,trans*-[RuL<sub>2</sub>(PPh<sub>3</sub>)<sub>2</sub>]PF<sub>6</sub>·CH<sub>2</sub>Cl<sub>2</sub>

complexes of the type [ML'<sub>2</sub>(PPh<sub>3</sub>)<sub>2</sub>] (M = Ru or Os)<sup>5a,12–14</sup> the two PC<sub>3</sub> fragments lie staggered when viewed down the PP axis (inset in Fig. 2) thereby reducing the PPh<sub>3</sub>...PPh<sub>3</sub> repulsion inherent in the *cis* configuration.

The average Ru–O bond length, 1.999(6) Å, in *trans,trans,trans*-[RuL<sub>2</sub>(PPh<sub>3</sub>)<sub>2</sub>]<sup>+</sup> is ca. 0.1 Å shorter than that, 2.095(6) Å, in *cis,trans,cis*-[RuL<sub>2</sub>(PPh<sub>3</sub>)<sub>2</sub>] due to the electrostatic effect of the greater charge in the trivalent ion. Significantly, the trend of Ru–O bond lengths in [Ru<sup>III</sup>(H<sub>2</sub>O)<sub>6</sub>]<sup>3+</sup>, 2.029(7) Å, and [Ru<sup>II</sup>(H<sub>2</sub>O)<sub>6</sub>]<sup>2+</sup>, 2.122(16) Å, is similar.<sup>15</sup> The Ru–N bond lengths also decrease in going from *cis,trans,cis*-[RuL<sub>2</sub>(PPh<sub>3</sub>)<sub>2</sub>] to *trans,trans,trans*-[RuL<sub>2</sub>(PPh<sub>3</sub>)<sub>2</sub>]<sup>+</sup> but the change is less dramatic. In contrast the average Ru–P bond length increases by a remarkable ca. 0.15 Å between the bivalent *cis,trans,cis* and trivalent *trans,trans,trans* forms. We note that in certain structurally characterised variable-valence [OsL'<sub>2</sub>(PPh<sub>3</sub>)<sub>2</sub>]<sup>2</sup> complexes the Os–P bond length increases respectively by ca. 0.04 and ca. 0.14 Å in going from the bivalent-*cis* to the bivalent-*trans* and trivalent-*trans* forms.<sup>12–14</sup> By analogy, we propose that the major part of the increase of ca. 0.15 Å noted above arises from the change in the oxidation state of ruthenium. This is consistent with 4dπ–3dπ Ru–P back-bonding which is much stronger in bivalent than in trivalent ruthenium.<sup>16</sup> The effect is evidently powerful enough to go far past offsetting the electrostatic factor noted above. A reduction in Ru–P back-bonding may be expected to cause a decrease in the length of the P–C bonds and an increase in the C–P–C angles within the PPh<sub>3</sub> fragments.<sup>17</sup> The ranges of the observed values are: *cis,trans,cis*-[RuL<sub>2</sub>(PPh<sub>3</sub>)<sub>2</sub>] 1.823(10)–1.857(9) Å and 98.6(4)–103.7(5)°, *trans,trans,trans*-[RuL<sub>2</sub>(PPh<sub>3</sub>)<sub>2</sub>]PF<sub>6</sub> 1.809(9)–1.835(12) Å and 99.7(5)–108.5(5)°. Unfortunately these ranges overlap considerably. The average values (1.84 Å and 102° for *cis,trans,cis*-Ru<sup>II</sup> and 1.82 Å and 104° for *trans,trans,trans*-Ru<sup>III</sup>) however have the correct trend although the differences are small.

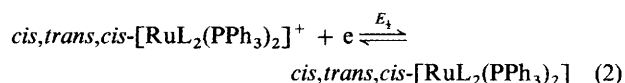
**Redox Behaviour.**—The electroactivity of the complexes was examined at a platinum electrode in dichloromethane solution. A one-electron quasi-reversible (peak-to-peak separation 90 mV) cyclic voltammetric response is displayed by each species. Although single crystals for the X-ray diffraction work could not be obtained in the case of *trans,trans,trans*-[RuL<sub>2</sub>(PPh<sub>3</sub>)<sub>2</sub>],

its cyclic voltammetric behaviour clearly establishes that it has the same isomeric geometry as the *trans,trans,trans*-Ru<sup>III</sup> complex. The voltammograms of the two species are superimposable, the initial scan being respectively anodic and cathodic for the bivalent and the trivalent states. The electrode reaction is as stated in equation (1). The value of



$E_1(\textit{trans,trans,trans})$  is –0.245 V vs. the ferrocene–ferrocene couple. Upon coulometry at 0.10 V, [RuL<sub>2</sub>(PPh<sub>3</sub>)<sub>2</sub>] is quantitatively oxidised to [RuL<sub>2</sub>(PPh<sub>3</sub>)<sub>2</sub>]<sup>+</sup>. The reverse process can be achieved by performing coulometry at –0.50 V. In both cases the coulomb counts correspond within experimental error to the transfer of one electron.

The  $E_1$  of the equation (2) couple corresponding to



*cis,trans,cis*-[RuL<sub>2</sub>(PPh<sub>3</sub>)<sub>2</sub>] is –0.095 V. It is thus 150 mV more positive than that of the equation (1) couple. Upon coulometric oxidation of *cis,trans,cis*-[RuL<sub>2</sub>(PPh<sub>3</sub>)<sub>2</sub>] at 0.20 V, one electron is transferred, but the product is found (from cyclic voltammetry, electronic and EPR spectra) to be *trans,trans,trans*-[RuL<sub>2</sub>(PPh<sub>3</sub>)<sub>2</sub>]<sup>+</sup>. Thus the *cis,trans,cis*-[RuL<sub>2</sub>(PPh<sub>3</sub>)<sub>2</sub>]<sup>+</sup> complex, although observable on the cyclic voltammetric time-scale, is not stable and undergoes isomerisation to the *trans,trans,trans* form during coulometry.

The equation (1) and (2) couples are of the d<sup>5</sup>–d<sup>6</sup> type. It is known from both theory and experiment that in pseudooctahedral complexes incorporating a pair of π-accepting ligand sites the  $E_1$  of d<sup>5</sup>–d<sup>6</sup> couples generally follow the trend *cis* > *trans* due to the stronger back-bonding in the d<sup>6</sup> (reductant) *cis* configuration.<sup>1c,2,12–14,18</sup> The inequality of  $E_1(\textit{cis,trans,cis}) > E_1(\textit{trans,trans,trans})$  fits well into this pattern.

**Geometrical Selection.**—Of the five possible geometrical forms (*trans,cis,cis* and *cis,cis,cis*, in addition to *cis,cis,trans*, *cis,trans,cis* and *trans,trans,trans*), only the latter two are

observed and isolated in the case of the bivalent metal. The trivalent complex is stable only in the *trans,trans,trans* form. These findings can be rationalised on the basis of the following three factors: (i) Ru–P back-bonding in the bivalent state (virtually absent in the trivalent state) for both *cis* and *trans* configurations of the  $\text{Ru}(\text{PPh}_3)_2$  motif, but in the order *cis* > *trans*; (ii)  $\text{PPh}_3 \cdots \text{PPh}_3$  steric repulsion which is much stronger in the *cis* than in the *trans*  $\text{Ru}(\text{PPh}_3)_2$  motif; and (iii) repulsion between  $\text{L}^-$  phenolato oxygen atoms bearing the anionic charges, the effect being stronger in the *cis*- compared to the *trans*- $\text{O}_2$  configuration.

Factors (i) and (ii) have been well documented<sup>5a,12–14</sup> for species of the type  $[\text{ML}'_2(\text{PPh}_3)_2]^z$  ( $\text{M} = \text{Ru}$  or  $\text{Os}$ ,  $\text{L}' = \text{SS}$  donor). The bivalent complex can thus have both *cis* and *trans* phosphine configurations. The isolation of  $[\text{RuL}_2(\text{PPh}_3)_2]$  in the *cis,trans,cis* and *trans,trans,trans* forms is therefore not unexpected. Both these isomers have *trans*- $\text{O}_2$  configurations and this is in line with (iii). The three isomers not observed in this work all have a *cis*- $\text{O}_2$  disposition. For the trivalent state, the *cis*-( $\text{PPh}_3$ )<sub>2</sub> [(i) and (ii)] and *cis*- $\text{O}_2$  [(iii)] configurations are destabilised. The only geometry that is not adversely affected is the *trans,trans,trans* one.

The  $[\text{RuL}_2(\text{PPh}_3)_2]^z$  system thus provides a fascinating example of geometrical selection: of the ten possible forms (the two oxidation states together) seven are not expressed as stable entities due to specific metal–ligand and ligand–ligand interactions.

## Conclusion

In search of factors controlling isomeric stability the  $[\text{RuL}_2(\text{PPh}_3)_2]^z$  family incorporating an unsymmetrical bidentate ligand ( $\text{L}^-$ ) has been scrutinised. Of the ten (five for each oxidation state) possible geometrical isomers, only two (*cis,cis,trans* and *trans,trans,trans*) for the bivalent ( $z = 0$ ) and one (*trans,trans,trans*) for the trivalent ( $z = +1$ ) states respectively could be isolated. The remarkable selectivity follows a simple pattern: (i) a *cis* or *trans* placement of the  $\text{PPh}_3$  pair for  $\text{Ru}^{\text{II}}$ , but only *trans* for  $\text{Ru}^{\text{III}}$ , and (ii) the phenolato oxygen atoms are *trans* for both  $\text{Ru}^{\text{II}}$  and  $\text{Ru}^{\text{III}}$ . The rationale for this pattern is provided by  $\text{Ru}^{\text{II}}$ –P back-bonding,  $\text{PPh}_3 \cdots \text{PPh}_3$  crowding and phenolato oxygen repulsion. The crystal structures of *cis,trans,cis*- $[\text{RuL}_2(\text{PPh}_3)_2]$  and *trans,trans,trans*- $[\text{RuL}_2(\text{PPh}_3)_2]\text{PF}_6 \cdot \text{CH}_2\text{Cl}_2$  have revealed amongst other things the importance of  $\text{Ru}^{\text{II}}$ –P back-bonding, with the trivalent complex ( $t_2^5$ ,  $S = \frac{1}{2}$ ) displaying a rhombic EPR spectrum. The  $\text{Ru}^{\text{III}}$ – $\text{Ru}^{\text{II}}$  reduction potential of the *cis,trans,cis* couple is significantly higher than that of the *trans,trans,trans* couple in accord with superior back-bonding in the *cis*- $\text{Ru}^{\text{II}}(\text{PPh}_3)_2$  motif.

## Experimental

**Materials.**—Commercial ruthenium trichloride was received from Arora Matthey, Calcutta, India and purified by repeated evaporation to dryness with concentrated hydrochloric acid. The compound  $[\text{Ru}(\text{PPh}_3)_3\text{Cl}_2]$  was prepared according to the reported procedure<sup>19</sup> and 8-hydroxyquinoline was purchased from Aldrich. The preparation of tetraethylammonium perchlorate and the purification of solvents for electrochemical and spectroscopic work were done as before.<sup>20,21</sup> All other chemicals and solvents were of reagent grade and used without further purification.

**Physical Measurements.**—UV/VIS/NIR spectra were recorded on a Hitachi 330 spectrophotometer. The magnetic susceptibility was measured on a PAR 155 vibrating-sample magnetometer fitted with a Walker Scientific magnet. The X-band EPR spectrum was recorded on a Varian E-109C spectrometer fitted with a quartz Dewar flask for measurements at 77 K (liquid nitrogen) and calibrated with respect to diphenylpicrylhydrazyl ( $g = 2.0037$ ). Electrochemical measurements were done at a platinum working electrode by using a

**Table 4** Crystallographic data for *cis,trans,cis*- $[\text{RuL}_2(\text{PPh}_3)_2]$  and *trans,trans,trans*- $[\text{RuL}_2(\text{PPh}_3)_2]\text{PF}_6 \cdot \text{CH}_2\text{Cl}_2$ <sup>a</sup>

Formula	<i>cis,trans,cis</i> - $[\text{RuL}_2(\text{PPh}_3)_2]$	<i>trans,trans,trans</i> - $[\text{RuL}_2(\text{PPh}_3)_2]\text{PF}_6 \cdot \text{CH}_2\text{Cl}_2$
$\text{C}_{54}\text{H}_{44}\text{N}_2\text{O}_2\text{P}_2\text{Ru}$		$\text{C}_{55}\text{H}_{44}\text{Cl}_2\text{F}_6\text{N}_2\text{O}_2$
<i>M</i>	913.9	1143.8
Crystal system	Monoclinic	Triclinic
Crystal size/mm	0.44 × 0.32 × 0.16	0.32 × 0.22 × 0.10
Space group	$P2_1/n$	$P\bar{1}$
<i>a</i> /Å	12.363(5)	11.208(4)
<i>b</i> /Å	17.495(8)	12.562(4)
<i>c</i> /Å	20.002(6)	19.988(8)
$\alpha/^\circ$	90	78.73(3)
$\beta/^\circ$	92.36(3)	81.09(3)
$\gamma/^\circ$	90	69.19(3)
<i>U</i> /Å <sup>3</sup>	4323(3)	2569(2)
<i>Z</i>	4	2
<i>F</i> (000)	1880	1162
<i>D<sub>c</sub></i> /g dm <sup>−3</sup>	1.404	1.479
$\mu/\text{cm}^{-1}$	4.71	5.68
2 $\theta$ range/ $^\circ$	2–50	2–48
No. of reflections collected	8244	8502
No. of unique reflections	7568	8032
No. of observed reflections [ <i>I</i> > 3 $\sigma$ ( <i>I</i> )]	3394	3563
Transmission factor <sup>b</sup>	0.84	0.89
Final <i>R</i> <sup>c</sup>	0.0682	0.0573
Final <i>R'</i> <sup>d</sup>	0.0650	0.0616
Goodness of fit <sup>e</sup>	1.72	1.11
Largest difference peak/e Å <sup>−3</sup>	0.81	0.63

<sup>a</sup> Details in common: *T* = 295 K,  $\lambda(\text{Mo-K}\alpha) = 0.710\,73\,\text{\AA}$ . <sup>b</sup> Maximum value normalised to 1. <sup>c</sup>  $R = \sum ||F_o| - |F_c|| / \sum |F_o|$ . <sup>d</sup>  $R' = [\sum w(|F_o| - |F_c|)^2 / \sum w|F_o|^2]^{1/2}$ ;  $w^{-1} = \sigma^2|F_o| + g|F_o|^2$ ;  $g = 0.0001$ . <sup>e</sup> The goodness of fit is defined as  $[\sum (|F_o| - |F_c|)^2 / (n_o - n_v)]^{1/2}$  where  $n_o$  and  $n_v$  denote the number of data and variables respectively.

PAR model 370-4 electrochemistry system as described elsewhere.<sup>12</sup> All experiments were performed under a dinitrogen atmosphere. Dichloromethane (0.1 mol dm<sup>−3</sup> in tetraethylammonium perchlorate) was used as the solvent with ferrocene as the internal standard. The reported potentials are referenced to the ferrocenium–ferrocene couple (found to have an  $E_1^\circ$  of 0.160 V vs. the saturated calomel electrode). Solution electrical conductivity was measured by using a Philips PR 9500 bridge. Microanalytical data (C, H and N) were obtained with the use of a Perkin-Elmer model 240C elemental analyser.

**Preparation of the Complexes.**—*cis,trans,cis*- and *trans,trans,trans*-Bis(8-hydroxyquinolinato)bis(triphenylphosphine)ruthenium(II). To a warm solution of  $[\text{Ru}(\text{PPh}_3)_3\text{Cl}_2]$  (100 mmol) in ethanol (30 cm<sup>3</sup>) was added 8-hydroxyquinoline (35 mg, 0.24 mmol). The mixture was refluxed for 1 h. Upon cooling, the yellow-green *trans,trans,trans* isomer separated as a microcrystalline solid which was collected by filtration, washed thoroughly with water and ethanol and dried *in vacuo* over  $\text{P}_4\text{O}_{10}$ . Yield 45%. The red filtrate was evaporated to dryness under reduced pressure, the residue was dissolved in a minimum volume of dichloromethane and was then subjected to chromatography on a silica gel (60–120 mesh, BDH) column (20 × 1 cm). On elution with benzene a red band moved out fast and was collected. The red crystalline residue (yield 45%) obtained by evaporation of solvent was the *cis,trans,cis* isomer.

*trans,trans,trans*-Bis(8-hydroxyquinolinato)bis(triphenylphosphine)ruthenium(III) hexafluorophosphate. To a solution of pure *cis,trans,cis*- or *trans,trans,trans*- $[\text{RuL}_2(\text{PPh}_3)_2]$  (100 mg, 0.11 mmol) in dichloromethane–acetonitrile (1:1, 30 cm<sup>3</sup>) was



**Table 5** Atomic coordinates ( $\times 10^4$ ) for *cis,trans,cis*-[RuL<sub>2</sub>(PPh<sub>3</sub>)<sub>2</sub>]

Atom	x	y	z	Atom	x	y	z
Ru	1522(1)	2094(1)	392(1)	C(25)	3821(8)	2272(6)	-606(5)
P(1)	3341(2)	2356(1)	257(1)	C(26)	4455(8)	2824(7)	-902(6)
P(2)	887(2)	2407(2)	-684(1)	C(27)	4794(9)	2712(8)	-1548(6)
O(1)	1026(5)	3173(3)	710(3)	C(28)	4525(10)	2067(9)	-1884(6)
O(2)	1856(6)	925(4)	274(3)	C(29)	3886(11)	1522(8)	-1606(6)
N(1)	-82(7)	1858(5)	623(4)	C(30)	3533(9)	1628(6)	-963(6)
N(2)	1917(6)	1794(5)	1384(4)	C(31)	3923(8)	3259(5)	549(5)
C(1)	-638(9)	1213(7)	531(6)	C(32)	5042(8)	3370(6)	570(5)
C(2)	-1713(10)	1136(9)	742(7)	C(33)	5489(8)	4065(6)	773(5)
C(3)	-2191(11)	1744(10)	1034(8)	C(34)	4841(10)	4666(6)	942(5)
C(4)	-1645(9)	2438(9)	1144(6)	C(35)	3740(10)	4554(6)	946(6)
C(5)	-2044(11)	3086(10)	1467(7)	C(36)	3269(9)	3855(5)	746(5)
C(6)	-1458(12)	3722(9)	1521(7)	C(37)	1643(7)	3136(5)	-1120(5)
C(7)	-397(10)	3779(7)	1285(6)	C(38)	1905(8)	3797(6)	-768(5)
C(8)	65(8)	3155(7)	967(5)	C(39)	2451(9)	4392(6)	-1058(6)
C(9)	-560(8)	2479(7)	924(5)	C(40)	2768(9)	4333(7)	-1706(7)
C(10)	1970(8)	2244(7)	1912(6)	C(41)	2527(9)	3683(7)	-2065(6)
C(11)	2258(9)	1963(9)	2558(6)	C(42)	1972(8)	3080(6)	-1778(5)
C(12)	2491(10)	1214(9)	2641(7)	C(43)	594(8)	1680(5)	-1332(5)
C(13)	2428(9)	706(8)	2097(6)	C(44)	857(9)	936(6)	-1211(5)
C(14)	2696(11)	-68(9)	2121(7)	C(45)	604(11)	384(6)	-1709(6)
C(15)	2643(12)	-500(8)	1556(8)	C(46)	87(10)	576(7)	-2305(5)
C(16)	2357(11)	-182(7)	921(7)	C(47)	-199(9)	1325(7)	-2410(6)
C(17)	2108(9)	589(6)	847(7)	C(48)	41(8)	1877(6)	-1931(6)
C(18)	2133(8)	1037(7)	1453(5)	C(49)	-483(7)	2841(6)	-656(4)
C(19)	4257(8)	1699(5)	729(6)	C(50)	-628(8)	3608(6)	-556(6)
C(20)	4709(12)	1055(7)	463(7)	C(51)	-1663(10)	3902(7)	-460(6)
C(21)	5291(14)	552(7)	858(8)	C(52)	-2540(10)	3422(8)	-505(6)
C(22)	5452(11)	664(7)	1537(8)	C(53)	-2418(9)	2649(8)	-620(6)
C(23)	5046(9)	1315(7)	1800(6)	C(54)	-1386(8)	2356(6)	-696(5)
C(24)	4463(8)	1833(6)	1412(5)				

**Table 6** Atomic coordinates ( $\times 10^4$ ) for *trans,trans,trans*-[RuL<sub>2</sub>(PPh<sub>3</sub>)<sub>2</sub>]PF<sub>6</sub>-CH<sub>2</sub>Cl<sub>2</sub>

Atom	x	y	z	Atom	x	y	z
Ru(1)	0	0	0	C(29)	3015(11)	-2536(9)	5436(7)
P(1)	1800(3)	-1114(2)	687(1)	C(30)	2777(12)	-2560(10)	4777(8)
O(1)	-1091(6)	161(5)	892(3)	C(31)	3183(10)	-1875(9)	4213(6)
N(1)	-496(7)	-1471(6)	113(4)	C(32)	3039(12)	-1851(12)	3521(8)
C(1)	-86(11)	-2323(8)	-254(5)	C(33)	3423(13)	-1125(12)	3023(7)
C(2)	-592(12)	-3232(9)	-110(5)	C(34)	4035(11)	-412(10)	3162(6)
C(3)	-1524(13)	-3244(10)	405(6)	C(35)	4266(10)	-437(8)	3822(5)
C(4)	-1962(10)	-2373(9)	832(5)	C(36)	3822(9)	-1171(8)	4347(5)
C(5)	-2886(11)	-2308(11)	1393(6)	C(37)	3014(9)	2554(8)	5718(4)
C(6)	-3216(11)	-1426(11)	1758(6)	C(38)	3491(10)	3354(8)	5297(5)
C(7)	-2637(10)	-580(9)	1617(5)	C(39)	3732(11)	4193(9)	5572(5)
C(8)	-1726(10)	-592(8)	1068(4)	C(40)	3456(11)	4233(10)	6255(6)
C(9)	-1412(9)	-1480(8)	660(5)	C(41)	2935(11)	3490(10)	6673(6)
C(10)	2410(10)	-164(8)	1011(5)	C(42)	2729(10)	2628(9)	6405(5)
C(11)	1596(10)	650(8)	1404(5)	C(43)	1867(9)	713(8)	5878(5)
C(12)	2048(12)	1443(10)	1614(6)	C(44)	778(10)	618(9)	5673(5)
C(13)	3236(12)	1444(10)	1413(6)	C(45)	109(12)	-50(10)	6080(6)
C(14)	4056(13)	662(10)	1012(6)	C(46)	541(11)	-617(9)	6713(6)
C(15)	3653(11)	-148(9)	802(5)	C(47)	1587(11)	-546(9)	6930(6)
C(16)	3209(10)	-2154(8)	326(5)	C(48)	2271(10)	115(8)	6515(5)
C(17)	3363(10)	-2286(8)	-362(5)	C(49)	1742(10)	2378(8)	4663(5)
C(18)	4470(11)	-3110(10)	-632(6)	C(50)	676(11)	3255(10)	4848(6)
C(19)	5400(13)	-3776(11)	-199(6)	C(51)	-193(12)	2945(10)	4370(6)
C(20)	5260(12)	-3682(10)	470(6)	C(52)	-17(12)	3738(10)	3729(6)
C(21)	4176(11)	-2871(10)	746(6)	C(53)	1038(12)	2864(11)	3528(7)
C(22)	1308(10)	-2017(8)	1427(5)	C(54)	1945(11)	2164(9)	3986(5)
C(23)	939(11)	-1701(10)	2080(6)	P(3)	7908(3)	3861(3)	1986(2)
C(24)	485(13)	-2429(11)	2613(7)	F(1)	8051(10)	4217(6)	1186(4)
C(25)	390(14)	-3412(12)	2488(7)	F(2)	7023(12)	3208(11)	1917(5)
C(26)	752(12)	-3751(11)	1873(6)	F(3)	7727(10)	3514(7)	2776(3)
C(27)	1226(12)	-3035(10)	1331(6)	F(4)	9013(10)	2728(8)	1928(5)
Ru(2)	5000	0	5000	F(5)	6766(11)	4999(8)	2044(4)
P(2)	2843(3)	1451(2)	5295(1)	F(6)	8734(14)	4549(12)	2069(7)
O(2)	4839(7)	213(6)	3998(3)	C(1S)	3896(22)	4632(27)	2674(14)
N(2)	4068(8)	-1151(6)	4999(4)	Cl(1S)	3539(9)	4840(6)	3504(4)
C(28)	3702(11)	-1835(8)	5528(6)	Cl(2S)	4062(14)	3154(15)	2665(7)

added cerium(IV) ammonium sulfate (100 mg, 0.16 mmol) dissolved in water (5 cm<sup>3</sup>). The mixture was stirred magnetically for 15 min during which time the colour of the solution became red-brown. The reaction mixture was then filtered, the filtrate concentrated to 10 cm<sup>3</sup> under reduced pressure and a saturated solution of NH<sub>4</sub>PF<sub>6</sub> (10 cm<sup>3</sup>) was added to it. The red-brown solid thus obtained was collected by filtration, washed with water and dried *in vacuo* over P<sub>4</sub>O<sub>10</sub>, yield 95%.

Slow diffusion of a dichloromethane solution of *trans,trans*,*trans*-[RuL<sub>2</sub>(PPh<sub>3</sub>)<sub>2</sub>]PF<sub>6</sub> into hexane yielded single crystals of composition [RuL<sub>2</sub>(PPh<sub>3</sub>)<sub>2</sub>]PF<sub>6</sub>·CH<sub>2</sub>Cl<sub>2</sub> (Found: C, 57.8; H, 3.8; N, 1.2. Calc. for C<sub>55</sub>H<sub>44</sub>Cl<sub>2</sub>F<sub>6</sub>N<sub>2</sub>O<sub>2</sub>P<sub>3</sub>Ru: C, 57.7; H, 3.9; N, 1.2%).

**Reaction of [RuH<sub>2</sub>(PPh<sub>3</sub>)<sub>4</sub>] with HL.**—The reaction was carried out in a way similar to that reported<sup>6</sup> using [RuH<sub>2</sub>(PPh<sub>3</sub>)<sub>4</sub>] (0.10 g). The product consisted mostly of red crystals, but some yellow-green crystals also deposited upon solvent evaporation and cooling. The whole mass was subjected to chromatography on silica gel. A red band was eluted with benzene and a green band with benzene–acetonitrile (1:1). Evaporation of the solvent afforded red (yield 75%) and yellow-green (yield 10%) crystals which were respectively found to be the *cis,trans,cis* and *trans,trans,trans* isomer of [RuL<sub>2</sub>(PPh<sub>3</sub>)<sub>2</sub>].

**X-Ray Structure Determinations.**—Single crystals of *cis,trans,cis*-[RuL<sub>2</sub>(PPh<sub>3</sub>)<sub>2</sub>] and *trans,trans,trans*-[RuL<sub>2</sub>(PPh<sub>3</sub>)<sub>2</sub>]·PF<sub>6</sub>·CH<sub>2</sub>Cl<sub>2</sub> were grown at 298 K by slow diffusion of hexane into dichloromethane solutions of the complexes. Selected crystal data and data collection parameters are collected in Table 4. The unit-cell parameters in each case were determined by a least-squares fit of 30 machine-centred reflections (20 < 2θ < 30°). Data were collected on a Siemens R3m/V diffractometer using graphite-monochromated Mo-Kα radiation (λ = 0.710 73 Å) and were corrected for Lorentz and polarisation factors. Each data set was corrected for empirical absorption on the basis of azimuthal scans.<sup>22</sup> Two standard reflections monitored after each 98 reflections for both the cases showed no significant intensity variation.

Systematic absences led to the identification of space group P2<sub>1</sub>/n for the ruthenium(II) complex. The structure of the ruthenium(III) complex was successfully refined in P $\bar{1}$ . Both the structures were solved by the heavy-atom method, the positions of the metal ions being determined from Patterson maps and the remaining non-hydrogen atoms by successive Fourier-difference syntheses. The structures were then refined by full-matrix least-squares procedures. All non-hydrogen atoms excluding the triphenylphosphine carbon atoms for the ruthenium(III) complex, were refined anisotropically. Hydrogen atoms were included at their respective calculated positions with fixed isotropic thermal parameters (0.08 Å<sup>2</sup>) at the final cycle of refinement. Final residuals are given in Table 4. Atomic coordinates for the non-hydrogen atoms are collected in Tables 5 and 6. All computations regarding data collection, structure solution and refinement were carried out on a MicroVax II computer using the SHELXTL-PLUS program package.<sup>23</sup>

Additional material available from the Cambridge Crystallographic Data Centre comprises H-atom coordinates, thermal parameters and remaining bond lengths and angles.

## Acknowledgements

The crystal structures were determined at the National Single Crystal Diffractometer Facility, Department of Inorganic Chemistry, Indian Association for the Cultivation of Science. Financial support received from the Council of Scientific and Industrial Research, New Delhi, India, is gratefully acknowledged.

## References

- (a) D. H. Evans and K. M. O'Connell, in *Electroanalytical Chemistry. A Series of Advances*, ed. A. J. Bard, Marcel Dekker, New York, 1986, vol. 14, p. 113; (b) W. E. Geiger, *Prog. Inorg. Chem.*, 1985, **33**, 275; (c) B. E. Bursten and M. R. Green, *Prog. Inorg. Chem.*, 1988, **36**, 393.
- A. M. Bond, R. Colton, J. E. Kevekordes and P. Panagiotidou, *Inorg. Chem.*, 1987, **26**, 1430; A. M. Bond, T. W. Hambley, D. R. Mann and M. R. Snow, *Inorg. Chem.*, 1987, **26**, 2257 and refs. therein.
- A. Pramanik, N. Bag and A. Chakravorty, *Inorg. Chem.*, 1993, **32**, 811; P. Basu and A. Chakravorty, *Inorg. Chem.*, 1992, **31**, 4980 and refs. therein; P. Basu, S. Bhanja Choudhury, S. Pal and A. Chakravorty, *Inorg. Chem.*, 1989, **28**, 2680.
- N. Bag, G. K. Lahiri and A. Chakravorty, *J. Chem. Soc., Dalton Trans.*, 1990, 1557.
- (a) A. Pramanik, N. Bag, G. K. Lahiri and A. Chakravorty, *J. Chem. Soc., Dalton Trans.*, 1990, 3823; (b) M. Menon, A. Pramanik, S. Chattopadhyay, N. Bag and A. Chakravorty, unpublished work.
- R. O. Rosete, D. J. Cole-Hamilton and G. Wilkinson, *J. Chem. Soc., Dalton Trans.*, 1979, 1618.
- J. W. Steed and D. A. Tocher, *J. Chem. Soc., Dalton Trans.*, 1992, 2765; S. Gopinathan, K. Joseph and C. Gopinathan, *Indian J. Chem., Sect. A*, 1987, **26**, 128; S. Gopinathan, S. S. Deshpande and C. Gopinathan, *Z. Anorg. Allg. Chem.*, 1985, **527**, 203; K. Joseph, S. Gopinathan and C. Gopinathan, *Synth. React. Inorg. Metal-Organ. Chem.*, 1984, **14**, 1005; K. Joseph, S. S. Deshpande, S. A. Pardhy, I. R. Unny, S. K. Pandit, S. Gopinathan and C. Gopinathan, *Inorg. Chim. Acta*, 1984, **82**, 59; J. A. Van Doorn and P. W. N. M. Van Leeuwen, *J. Organomet. Chem.*, 1981, **222**, 299; P. Powell, *J. Organomet. Chem.*, 1974, **65**, 89.
- Y. Kamata, T. Kimura, R. Hirota, E. Miki, K. Mizumachi and T. Ishimori, *Bull. Chem. Soc. Jpn.*, 1987, **60**, 1343; H. Kamata, Y. Konishi, Y. Kamata, E. Miki, K. Mizumachi, T. Ishimori, T. Nagai and M. Tanaka, *Chem. Lett.*, 1988, **1**, 159.
- G. K. Lahiri, S. Bhattacharya, B. K. Ghosh and A. Chakravorty, *Inorg. Chem.*, 1987, **26**, 4324.
- N. E. Domracheva, V. N. Konstantinov, S. A. Luchkina and I. V. Ovchinnikov, *Koord. Khim.*, 1985, **11**, 503; G. S. Rodman and J. K. Nagle, *Inorg. Chim. Acta*, 1985, **105**, 205.
- S. Bhattacharya, *Polyhedron*, 1993, **12**, 235.
- A. Pramanik, N. Bag, D. Ray, G. K. Lahiri and A. Chakravorty, *Inorg. Chem.*, 1991, **30**, 410.
- A. Pramanik, N. Bag, D. Ray, G. K. Lahiri and A. Chakravorty, *J. Chem. Soc., Chem. Commun.*, 1991, 139; A. Pramanik, N. Bag, G. K. Lahiri and A. Chakravorty, *J. Chem. Soc., Dalton Trans.*, 1992, 101.
- A. Pramanik, N. Bag and A. Chakravorty, *J. Chem. Soc., Dalton Trans.*, 1993, 237.
- P. Bernhard, H. B. Burgi, J. Hauser, H. Lehmann and A. Ludi, *Inorg. Chem.*, 1982, **21**, 3936.
- H. Taube, *Pure Appl. Chem.*, 1979, **51**, 901; M. Sekine, W. D. Harman and H. Taube, *Inorg. Chem.*, 1988, **27**, 3604; D. E. Richardson, D. D. Walker, J. E. Sutton, K. O. Hodgson and H. Taube, *Inorg. Chem.*, 1979, **18**, 2216; J. F. Wishart, A. Bino and H. Taube, *Inorg. Chem.*, 1986, **25**, 3318.
- A. G. Orpen and N. G. Connelly, *Organometallics*, 1990, **9**, 1206.
- B. E. Bursten, *J. Am. Chem. Soc.*, 1982, **104**, 1299.
- T. A. Stephenson and G. Wilkinson, *J. Inorg. Nucl. Chem.*, 1966, **28**, 945.
- A. R. Chakravarty and A. Chakravorty, *Inorg. Chem.*, 1981, **20**, 275.
- A. R. Chakravarty and A. Chakravorty, *J. Chem. Soc., Dalton Trans.*, 1982, 615; S. Bhattacharya and A. Chakravorty, *Proc. Indian Acad. Sci., Chem. Sci.*, 1985, **95**, 159; A. K. Mahapatra, S. Datta, S. Goswami, M. Mukherjee, A. K. Mukherjee and A. Chakravorty, *Inorg. Chem.*, 1986, **25**, 1715.
- A. C. T. North, D. C. Philips and F. S. Mathews, *Acta Crystallogr., Sect. A*, 1968, **24**, 351.
- G. M. Sheldrick, SHELXTL-PLUS 90, Structure Determination Software Programs, Siemens Analytical X-Ray Instruments, Madison, WI, 1990.

Received 16th September 1994; Paper 4/05649C